

## Article

# Occurrence of and Factors Affecting Groundwater Fluoride in the Western Coastal Area of Hainan Island, South China

Ruinan Liu <sup>1,2</sup>, Xiwen Li <sup>3,\*</sup>, Xiujiu Yang <sup>3,\*</sup> and Ming Zhang <sup>4</sup> 

<sup>1</sup> Institute of Hydrogeology and Environmental Geology, Chinese Academy of Geological Sciences, Shijiazhuang 050061, China; liuruinan1996@163.com

<sup>2</sup> School of Environmental Studies, China University of Geosciences, Wuhan 430074, China

<sup>3</sup> Haikou Marine Geological Survey Center, China Geological Survey, Haikou 571127, China

<sup>4</sup> Faculty of Engineering, China University of Geosciences, Wuhan 430074, China; zhangming8157@126.com

\* Correspondence: lxw1818168@163.com (X.L.); yangxiuj9@163.com (X.Y.)

**Abstract:** Hainan, a well-known center of tropical agricultural production in south China, has received little attention regarding groundwater fluoride contamination. This study investigates the occurrence of fluoride in the western coastal area of Hainan Island and discusses factors affecting groundwater fluoride contamination in various aquifers and areas with different land-use types using hydrochemistry and multivariate statistical analysis. A total of 100 groundwater samples were collected from the western coastal area of Hainan Island. The results show that the groundwater fluoride concentration is as high as 4.18 mg/L and that F<sup>-</sup>-high (>1 mg/L) groundwater accounts for 9% of total groundwater. The proportion of F<sup>-</sup>-high fissure water is about two times that of F<sup>-</sup>-high pore water. Among the different land-use types, the proportion of F<sup>-</sup>-high groundwater from highest to lowest is as follows: bare land > cultivated land > woodland > construction land > grassland. The main factor affecting fluoride in pore water is the leaching of fluorine/aluminum-containing minerals such as phlogopite and calcite in the vadose zone, which is characterized by the co-enrichment of fluoride and aluminum in pore water. The leading cause of fluoride in fissure water is the leaching of fluorine-containing fertilizers, and continuous irrigation promotes the cation exchange of sodium, strontium, and calcium, which is characterized by the co-enrichment of fluoride with sodium and strontium in fissure water. Consequently, it is advised to minimize the excessive use of fluoride fertilizers and increase groundwater quality monitoring in order to decrease the emergence of F<sup>-</sup>-high groundwater in the western coastal area of Hainan Island.

**Keywords:** fluoride; groundwater; occurrence; factors; Hainan Island



**Citation:** Liu, R.; Li, X.; Yang, X.; Zhang, M. Occurrence of and Factors Affecting Groundwater Fluoride in the Western Coastal Area of Hainan Island, South China. *Water* **2023**, *15*, 3678. <https://doi.org/10.3390/w15203678>

Academic Editors: Juan José Durán, Cesar Andrade and Dimitrios E. Alexakis

Received: 17 July 2023

Revised: 21 September 2023

Accepted: 18 October 2023

Published: 20 October 2023



**Copyright:** © 2023 by the authors. Licensee MDPI, Basel, Switzerland. This article is an open access article distributed under the terms and conditions of the Creative Commons Attribution (CC BY) license (<https://creativecommons.org/licenses/by/4.0/>).

## 1. Introduction

Groundwater is a precious resource that provides drinking water for about 50% of the world's population [1–3]. In China, about one-third of water resources are groundwater, 70% of Chinese citizens drink groundwater, and 90% of urban domestic and industrial water depends on groundwater [4]. Therefore, groundwater is essential for sustaining human life, social progress, and the environment [5–7]. However, there has been a significant issue with groundwater quality in recent years. Fluoride is a common groundwater pollutant, and one study estimates that 200 million people worldwide are at risk of suffering groundwater fluorosis [8]. In China, thirty provinces (cities and districts) are affected by groundwater fluoride poisoning; most of these areas are located in the north, including areas such as the Songnen Plain, the North China Plain, and the Hexi Corridor Basin [4]. Long-term exposure to groundwater with a high fluoride level can impact a person's teeth, bones, and neurological system as well as induce symptoms of nausea, diarrhea, and abdominal pain [8,9]. Due to its high toxicity, fluoride poses a serious risk to human health even at very low concentrations [8].

Groundwater quality issues in Hainan Island, China's southernmost island, have previously received little attention. It is important to note that groundwater fluoride pollution in southern China, particularly in coastal areas, is frequently disregarded. Hainan Island is China's primary production base for tropical agriculture. On the one hand, the need for water resources for the socioeconomic growth of Hainan Province as a pilot free trade zone is increasing, and groundwater supplies are becoming a crucial issue. On the other hand, the standards for building a sustainable civilization are improving. To successfully support the ecological growth of civilization and groundwater safety in Hainan Province, it is necessary to identify the issues with groundwater quality. According to the results of the "Groundwater Resources Investigation and Evaluation Report of Hainan Province" implemented in 2021, the groundwater on Hainan Island shows significant nitrate pollution. However, the impact of fluoride on groundwater quality is still unclear. As a result, it is necessary to identify the status of fluoride contamination in groundwater on Hainan Island.

This study intends to (i) describe the concentration of fluoride in groundwater in various aquifers and land-use types in the western coastal area of Hainan Island, China; (ii) delineate the spatial distribution of fluoride; and (iii) discuss the factors affecting fluoride concentrations in various aquifers and land-use types. The findings provide a scientific foundation for groundwater pollution prevention and control on Hainan Island as well as a guide for managing groundwater resources on other sizable tropical islands around the world that are comparable to Hainan Island. The results reveal for the first time the occurrence of and factors affecting fluoride in groundwater in the western coastal area of Hainan Island.

## 2. Study Area

### 2.1. Geographical Overview and Land-Use Types

Hainan Island is located in the south of China. The study area covers about 900 km<sup>2</sup> and is located in the NW coastal area of Hainan Island (108°37'–108°59' E, 19°9'–19°30'71' N) and includes the six major towns: Sigeng, Changhua, Haiwei, Shiyuetian, Wulie, and Sanjia (Figure 1). The mean elevations of the western and eastern parts of the study area are about 15 m and 150 m, respectively. Based on remote sensing interpretation, the land-use types in the study area were divided into seven main categories, namely, water bodies, bare land, cultivated land, construction land, grassland, shrubs, and trees. In this case, shrubs and trees were defined as woodland. By area estimates, woodland and grassland account for the largest share of land-use types, followed by construction land and cultivated land accounting for 20% and 10%, respectively; water bodies and bare land account for the least share. Woodland and grassland are mainly distributed in the mountainous areas of Changhua Daling and Sanjialing, construction land is mainly distributed on both sides of the downstream regions of the Changhua River and Sigeng town, and cultivated land is sporadically distributed across the whole district (Figure S1).

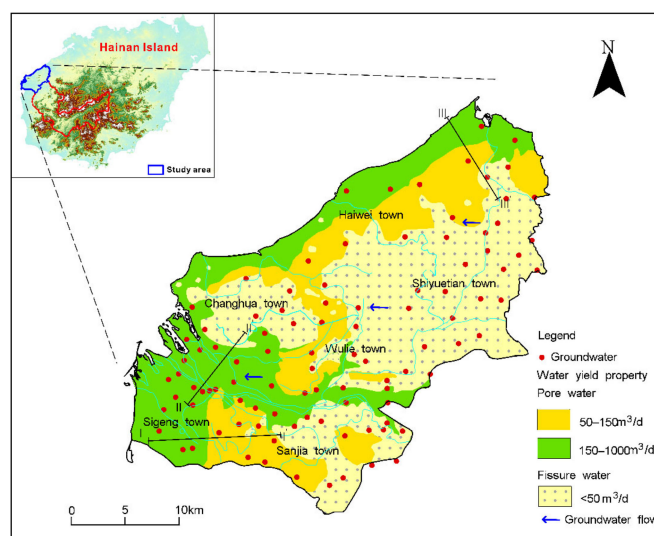


**Figure 1.** Hydrogeological division and sampling sites in the western coastal area of Hainan Island.

## 2.2. Geological and Hydrogeological Conditions

The study area is dominated by Middle Proterozoic, Silurian, Carboniferous, Cretaceous, and Quaternary strata in addition to a large distribution of intrusive rocks (Figure S2). Among them, the rock types are mainly biotite plagioclase gneiss, mixed granodiorite, metamorphosed quartz sandstone, sericite slate interbedded with tuff lenses, sericite kyanite, quartz sandstone, silty sandstone, and conglomerate. The acidic-medium acidic intrusive rocks are mainly black mica granite. The lithology of the Quaternary is mainly gravel, sand, clay, and beach rock. The topography of the study area is generally high in the east and low in the west, sloping from east to west. The coastal plains in the west and the mountain plains in the east account for more than 40% of the area, while the rest of the area comprises terraces and hilly areas, mostly distributed in the town of Changhua and the border areas of Haiwei, Shiyuetian, and Wulie. Groundwater in the study area is divided into two categories: pore water of the loose rock type of the Quaternary and bedrock fissure water (Figure 1). A loose rock aquifer is distributed mainly in the coastal accumulation layer, the river alluvial deposit, and the mountain front erosion accumulation layer. The lithology is mainly shell-containing medium-fine sand, gravelly sandy soil, medium-coarse sand, sand, and gravel (Figure S1). The thickness of the aquifer is about 5–15 m and the depth of the water table is 0–2 m. According to the Hainan Island Uniform Survey Report, the specific yield of the medium sand is about 0.2, and the recharge coefficient of precipitation is about 0.471. Furthermore, the area is well watered, and the water yield properties are 50–150 m<sup>3</sup>/d and 150–1000 m<sup>3</sup>/d. The bedrock fissure water is mainly distributed in the Changhua Daling and Sanjialing mountainous areas, with loose stratum lithology and high permeability. However, the groundwater is poorly enriched, and the water yield property is less than 50 m<sup>3</sup>/d. In addition, the annual average precipitation and evaporation in the study area are 1150 mm and 2419 mm, respectively. Moreover, the groundwater in the area is mainly recharged by precipitation and discharged by springs or evaporation. In the Piedmont area, the water table depth of unconfined water is generally higher than that of the confined water, resulting in lateral recharge of confined water by unconfined water.

## 3. Materials and Methods

### 3.1. Sampling and Analysis

A total of 100 groundwater samples including 51 pore water (PW) and 49 fissure water (FW) were collected in the study area in 2022 (Figure 1). They were collected at a density of 8–12 per 100 km<sup>2</sup> in the plains areas and 3–6 per 100 km<sup>2</sup> in the hilly areas. The samples were stored at a low temperature (4 °C) and sent to the laboratory for testing. pH, dissolved oxygen (DO), and the oxidation–reduction potential (ORP) were tested using a

multi-parameter water quality tester (DZB-712F) at the sampling site after calibration of the instrument.  $\text{HCO}_3^-$  was measured by the titration method;  $\text{NH}_4^+$  by ion chromatography (AQ-1100 ion chromatograph);  $\text{F}^-$ ,  $\text{NO}_3^-$ ,  $\text{Cl}^-$ , and  $\text{SO}_4^{2-}$  by ion chromatography (ion chromatography Aqion);  $\text{NO}_2^-$  by spectrophotometry (visible spectrophotometer 721N); total dissolved solids (TDS) by the weighing method (analytical balance SQP); arsenic (As) and selenium (Se) by the atomic fluorescence method (atomic fluorescence photometer AFS-9800); and  $\text{K}^+$ ,  $\text{Na}^+$ ,  $\text{Ca}^{2+}$ ,  $\text{Mg}^{2+}$ , aluminum (Al), barium (Ba), manganese (Mn), and strontium (Sr) by inductively coupled plasma emission spectrometry (inductively coupled plasma emission spectrometer ICAP6300). Quality control of the water sample testing was implemented using blank samples, parallel samples, and spiked samples. Among them, the blank and parallel samples accounted for 10–30% of each batch of samples, the blank samples were detected, and the parallel samples were qualified. The recoveries of the spiked samples were 86–113%, which were also within the qualified range of 80–120%.

### 3.2. Inverse Distance Weighting (IDW) Method

The inverse distance weighting method is a simple and common spatial interpolation method, which is based on the principle that the closer the distance between two sample points is, the more similar the properties. It takes the distance between the point to be estimated and the known sample point as the weight for the weighted average, and the closer the sample point to be estimated is, the greater the weight given to the sample point. The brief steps are as follows: (i) determine the location to be interpolated and the location of the known sample points, and calculate the weight of each sample point based on the distance between the location to be interpolated and the known sample points; and (ii) use the weight of each sample point to perform a weighted average of its function value to obtain the interpolation result.

### 3.3. Principal Component Analysis (PCA) and Hierarchical Cluster Analysis (HCA)

The principal component analysis (PCA) method extracts the principal factor variables (PCs) by retaining the most important features of the high-dimensional raw data through the concept of dimensionality reduction. The rotation of principal factors is performed by the Varimax method. The principal factors with eigenvalues  $> 1$  are retained for analysis [10]. Hierarchical cluster analysis (HCA) is another multivariate statistical technique for analyzing multidimensional water chemistry datasets [11]. Its main concept is to cluster variables that are close to each other into classes first and those that are farther away into classes later, in order, until each variable is grouped into the appropriate class according to its distance. It can group chemical components of different origins and hydrogeochemical behavior [11]. In this study, principal component analysis and hierarchical cluster analysis were performed using SPSS<sup>®</sup> version 23.0 software (IBM Corp., Armonk, NY, USA).

## 4. Results

### 4.1. Fluoride Concentrations in Different Aquifers and Land-Use Types

As shown in Figure 2 and Table S1, a wide range of groundwater  $\text{F}^-$  concentrations in the western coastal area of Hainan Island from below the detection limit ( $< \text{DL}$ ) to 4.18 mg/L were found.  $\text{F}^-$ -high groundwater accounted for 9% of the total groundwater in the western coastal area of Hainan Island. The  $\text{F}^-$  concentrations of PW and FW ranged from  $< \text{DL}$  to 1.42 mg/L and  $< \text{DL}$  to 4.18 mg/L, respectively. The maximum concentration of  $\text{F}^-$  in FW was about three times that in PW. The mean value of  $\text{F}^-$  in FW was 0.58 mg/L, which was 2.3 times that in PW. Moreover, the  $\text{F}^-$  coefficients of variation (CVs) in PW and FW were 0.68 and 0.56 (Table S1), respectively, indicating that they have a more uniform spatial distribution of fluoride concentrations. The proportion of  $\text{F}^-$ -high groundwater (PFHG) in FW was 12.2%, which was about 2 times that in PW.

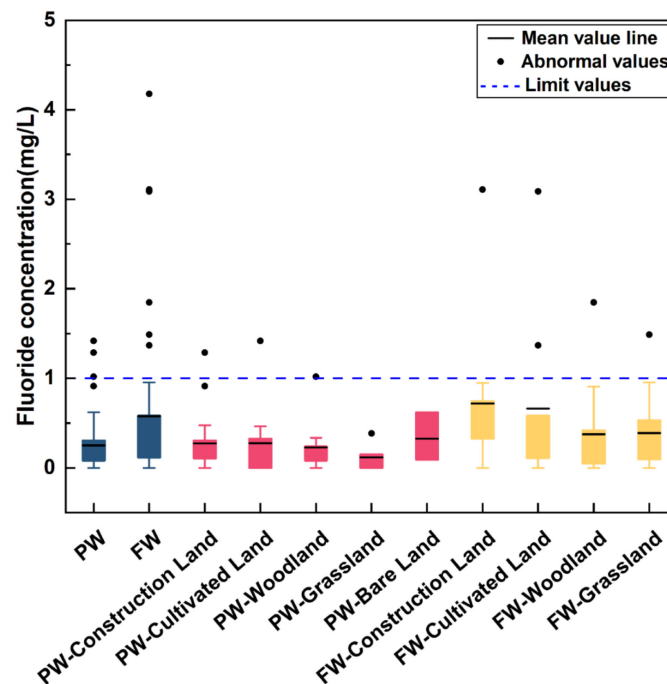
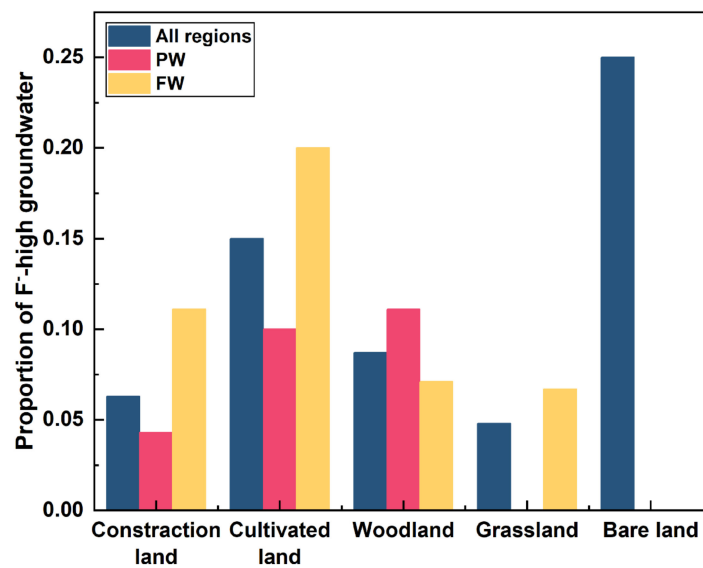


Figure 2. Groundwater fluoride concentrations in various aquifers and land-use types.

The fluoride concentrations in different land-use types are also shown in Figure 2. The  $F^-$  concentrations of PW in construction land, cultivated land, woodland, grassland, and bare land ranged from <DL to 1.29, <DL to 1.42, <DL to 1.02, <DL to 0.39, and 0.09 to 0.62 mg/L, respectively. In PW, the highest mean  $F^-$  concentration occurred in bare land, followed by cultivated land, construction land, woodland, and grassland. Compared to the CVs for other land-use types, the CVs for construction land and bare land were closer to 1, indicating a relatively high spatial dispersion of fluoride in construction land and bare land (Table S1). The PFHG values of woodland and cultivated land were the highest, with values of 11.1% and 10%, respectively, which were about 2.5 times that of construction land. However, there was no  $F^-$ -high groundwater in grassland and bare land (Figure 3). In FW, the  $F^-$  concentrations in construction land, cultivated land, woodland, and grassland ranged from <DL to 3.11, <DL to 3.09, <DL to 1.85, and <DL to 1.49 mg/L, respectively. The mean  $F^-$  concentration in construction land was 0.72 mg/L, while cultivated land, woodland, and grassland had relatively lower mean values of 0.66, 0.38, and 0.39 mg/L, respectively. The CV of grassland in FW was higher than that in construction land, cultivated land, and woodland (Table S1), indicating that the  $F^-$  concentration distribution in FW in grassland was relatively more discrete. Except for bare land (not statistically significant, as there was only one data point), the PFHG of cultivated land was the highest, with a value of 20%, which was about two times that of cultivated land and about three times that of woodland and grassland (Figure 3).



**Figure 3.** Proportion of F<sup>-</sup>-high groundwater in different land-use types.

#### 4.2. Hydrochemistry Characteristics of Groundwater with Different Levels of F<sup>-</sup>

As shown in Table 1, the pH of both F<sup>-</sup>-high and F<sup>-</sup>-poor groundwater in the study area was about 7. In PW, the average concentration order of major cations in F<sup>-</sup>-high groundwater was Na<sup>+</sup> > Ca<sup>2+</sup> > Mg<sup>2+</sup> > K<sup>+</sup>, while that of major cations in F<sup>-</sup>-poor groundwater was Ca<sup>2+</sup> > Na<sup>+</sup> > K<sup>+</sup> > Mg<sup>2+</sup>. Compared to F<sup>-</sup>-poor groundwater, F<sup>-</sup>-high groundwater had relatively high sulfate concentrations, with an average value that was about 1.2 times higher than that of F<sup>-</sup>-poor groundwater. The mean concentration order of major anions in F<sup>-</sup>-high groundwater was HCO<sub>3</sub><sup>-</sup> > SO<sub>4</sub><sup>2-</sup> > Cl<sup>-</sup>, while that of major anions in F<sup>-</sup>-poor groundwater was HCO<sub>3</sub><sup>-</sup> > Cl<sup>-</sup> > SO<sub>4</sub><sup>2-</sup>. Moreover, the mean value of NH<sub>4</sub><sup>+</sup> and NO<sub>2</sub><sup>-</sup> had no significant difference in F<sup>-</sup>-high and F<sup>-</sup>-poor groundwater. However, NO<sub>3</sub><sup>-</sup> and TDS of F<sup>-</sup>-high groundwater were relatively low, with mean values of 30.4 mg/L and 320.8 mg/L. In addition, the average concentrations of As, Se, and Ba in F<sup>-</sup>-high groundwater were larger compared to those in F<sup>-</sup>-poor groundwater, where the average concentration of Ba was about three times higher than that in F<sup>-</sup>-poor groundwater. By contrast, the average concentrations of Al, Mn, and Sr in F<sup>-</sup>-high groundwater were higher than those in F<sup>-</sup>-poor groundwater.

In FW, the average concentration order of major cations in F<sup>-</sup>-high groundwater was Na<sup>+</sup> > Ca<sup>2+</sup> > Mg<sup>2+</sup> > K<sup>+</sup>, while that of major cations in F<sup>-</sup>-poor groundwater was Ca<sup>2+</sup> > Na<sup>+</sup> > Mg<sup>2+</sup> > K<sup>+</sup>. Compared to F<sup>-</sup>-poor groundwater, the major anion contents of the F<sup>-</sup>-high groundwater were significantly different, with the average concentration order of HCO<sub>3</sub><sup>-</sup> > Cl<sup>-</sup> > SO<sub>4</sub><sup>2-</sup>. Moreover, the mean value of NH<sub>4</sub><sup>+</sup> and NO<sub>2</sub><sup>-</sup> had no significant difference in F<sup>-</sup>-high and F<sup>-</sup>-poor groundwater. However, the mean value of NO<sub>3</sub><sup>-</sup> in F<sup>-</sup>-poor groundwater was 1.5 times that in F<sup>-</sup>-high groundwater. And the mean value of TDS in F<sup>-</sup>-high groundwater was relatively higher at about 1.4 times that in F<sup>-</sup>-poor groundwater. In addition, the As, Mn, and Sr concentrations in F<sup>-</sup>-high groundwater were higher than those in F<sup>-</sup>-poor groundwater, and their average values were more than two times those in F<sup>-</sup>-poor groundwater. By contrast, the average concentrations of Se, Al, and Ba in F<sup>-</sup>-high groundwater were relatively lower than those in F<sup>-</sup>-poor groundwater.

**Table 1.** Mean values of hydrochemical parameters in groundwater with different levels of F<sup>-</sup>.

Groundwater	pH	K <sup>+</sup>	Na <sup>+</sup>	Ca <sup>2+</sup>	Mg <sup>2+</sup>	Cl <sup>-</sup>	SO <sub>4</sub> <sup>2-</sup>	HCO <sub>3</sub> <sup>-</sup>	NH <sub>4</sub> <sup>+</sup>
FHG in PW	7.3	7.4	44.1	44.0	14.0	38.2	55.1	128.0	0.1
FPG in PW	7.1	23.0	40.5	41.0	16.5	63.1	46.6	117.0	0.1
FHG in FW	7.1	2.3	95.6	53.2	18.1	108.1	37.5	242.8	<DL
FPG in FW	7.2	13.1	42.4	43.2	20.3	53.6	31.8	158.4	0.1
Groundwater	NO <sub>3</sub> <sup>-</sup>	NO <sub>2</sub> <sup>-</sup>	TDS	As	Se	Al	Ba	Mn	Sr
FHG in PW	30.4	<DL	320.8	0.9	0.3	0.9	0.1	0.1	0.4
FPG in PW	47.5	<DL	324.1	1.3	1.3	0.1	0.2	0.1	0.4
FHG in FW	29.7	<DL	442.9	5.7	0.5	<DL	0.1	0.1	0.8
FPG in FW	44.5	<DL	321.5	0.9	1.0	0.1	0.2	<DL	0.3

Notes: Except for pH, As (ug/L), and Se (ug/L), the units of other parameters are mg/L; FHG: F<sup>-</sup>-high (>1 mg/L); FPG: F<sup>-</sup>-poor (≤1 mg/L); DL: detection limit.

#### 4.3. Spatial Distribution of Fluoride

As shown in Figure 4, F<sup>-</sup>-high (>1 mg/L) groundwater accounted for about 5% of the study area distribution, mainly in the eastern part of Sanjia town, the southwestern part of Shiyuetian town, and the southeastern part of Wulie town, with a small amount in Haiwei town and Changhua town, while there was no F<sup>-</sup>-high groundwater in Sigeng town. In terms of different land-use types, F<sup>-</sup>-high groundwater was mainly found in bare land, with the proportion in descending order as follows: bare land (25%)> cultivated land (15%)> woodland (8.7%)> construction land (6.3%)> grassland (4.8%) (Figure 3).

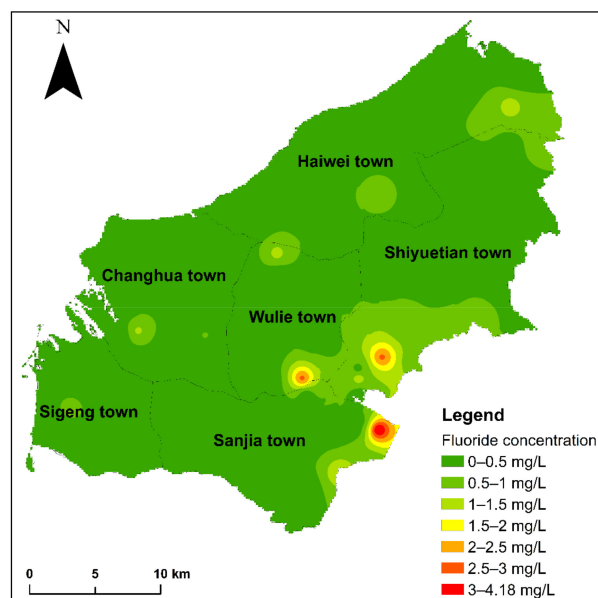


**Figure 4.** Spatial distribution of fluoride concentrations interpolated using the inverse distance weighting (IDW) method.

#### 4.4. PCA and HCA

As shown in Figure 5, the groundwater chemistry of PA and FA were both controlled by a six-factor model, and the six PCs accounted for 70.8% and 76.1% of the cumulative variance contribution, respectively. In PW, PC4 had moderate positive loading with F<sup>-</sup> and Al of 0.70 and 0.5, respectively (Figure 5a). Moreover, PC4 had a moderate negative loading with Ba of −0.67 (Figure 5a). In FW, PC3 had strong positive loading with F<sup>-</sup> and Sr of 0.89 and 0.84, respectively (Figure 5b), indicating that they have the same source or geochemical behavior [12]. In addition, PC3 had weak positive loading with Na<sup>+</sup> and weak negative loading with NO<sub>3</sub><sup>-</sup>, in which the loading was 0.37 and −0.31, respectively. Hierarchical cluster analysis for pore water and fissure water is shown in Figure 6. As shown in Figure 6a, the twenty groundwater chemical parameters were divided into

six clusters at a rescaled distance of 20. Among them,  $F^-$  was in a cluster with Al at a rescaled distance of 20. Similarly, as shown in Figure 6b, the twenty groundwater chemical parameters were divided into five clusters at a rescaled distance of 20. And  $F^-$  was in a cluster with Sr, at a rescaled distance of 10, indicating that  $F^-$  was more closely related to Sr in FW.

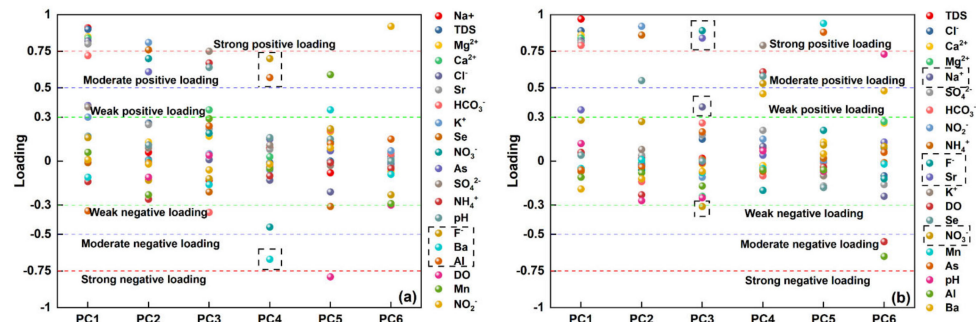


Figure 5. Factor loadings for principal component analysis of (a) pore water and (b) fissure water.

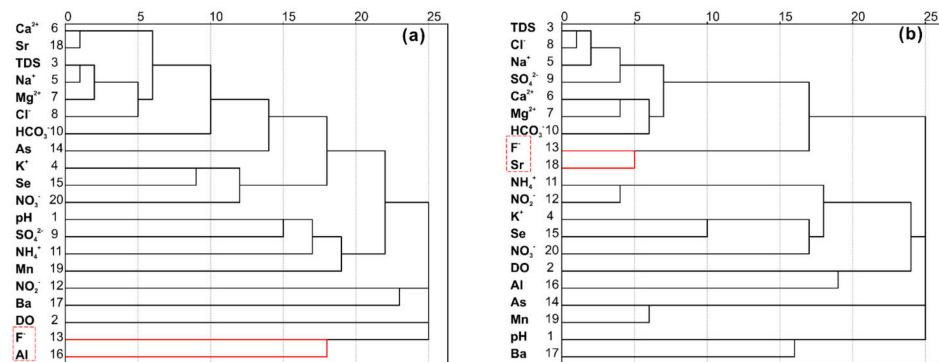


Figure 6. Hierarchical cluster analysis of (a) pore water and (b) fissure water.

### 5. Discussion

Both anthropogenic and natural factors frequently contribute to the occurrence of high groundwater fluoride levels. High levels of nitrate and total dissolved solids are frequent signs of different anthropogenic pollution inputs [13]. However, in this study, the  $F^-$ -high groundwater in the bare land was accompanied by low concentrations of nitrate (<1 mg/L) and total dissolved solids (<200 mg/L), indicating that the geological sources rather than anthropogenic contamination contributed to the  $F^-$ -high groundwater in bare land because fluoride-containing minerals such as fluorspar and calcite in the ground can dissolve and release fluoride into the groundwater under certain conditions [14]. Additionally, the proportion of  $F^-$ -high groundwater in cultivated land was two times or higher than that in other land-use types, except for bare land, indicating that long-term agricultural irrigation that causes soil fluoride to leach down and the use of fluoridated pesticides and fertilizers (such as fluoridated phosphate fertilizers) may be the main anthropogenic sources of groundwater fluoride in the study area [15,16]. As shown in Figure 3, the proportion of  $F^-$ -high groundwater in pore water was higher in woodland than in areas with high-intensity anthropogenic activities such as cultivated land and construction land, indicating that the  $F^-$ -high pore water in the study area may be mainly from geological sources rather than from anthropogenic contamination. By contrast, the proportion of  $F^-$ -high groundwater in fissure water was twice or more than that in other land-use types, indicating that the  $F^-$ -high fissure water in the study area may be more likely to originate from long-term agricultural irrigation resulting in soil fluoride leaching and infiltration and the use of fluoridated pesticides and fertilizers (such as fluoridated phosphate fertilizers).

According to Figure 5a, PC4 in pore water chemistry was characterized as a moderate positive loading of fluoride with aluminum and a moderate negative loading with barium.

Fluoride ions can react with aluminum ions in water instead of hydroxide ions under acidic or neutral conditions to generate aluminum fluoride ions such as  $\text{AlF}_2^+$ ,  $\text{AlF}_2^+$ ,  $\text{AlF}_4^-$ , and  $\text{AlF}_6^{3-}$  because, as demonstrated in previous research, fluoride ions are similar in size to hydroxide ions [17]. Correspondingly, the pH of the  $\text{F}^-$ -high pore water in the study area was mostly around 7. Therefore, the fact that fluoride and aluminum are located in the same factor indicated a co-existence relationship/co-source relationship between fluoride and aluminum in pore water, such as the dissolution of concurrent aluminum/fluoride-rich minerals like mica and hornblende [18]. The results of hierarchical cluster analysis, which demonstrated that pore water fluoride was most strongly related to aluminum, further corroborated this conclusion (Figure 6a). At the same time, the study area is mainly distributed with Middle Proterozoic, Silurian, Carboniferous, Cretaceous, and Quaternary strata, and there is also a large area of intrusive rock distribution. The main types of rocks are gneiss, amphibolite, granite, sericite slate, etc., which are rich in fluoride-containing minerals such as mica and hornblende, etc., which can also support the above conclusions. In addition, the fact that  $\text{F}^-$  and Ba were located in the same factor and had opposite loading relationships may indicate their opposing geochemical behavior since the co-precipitation of barium sulfate made the barium content in groundwater often be controlled by the groundwater sulfate concentration, and high-sulfate-concentration groundwater was often accompanied by low levels of barium [19–21]. Correspondingly, the average sulfate and barium concentrations in  $\text{F}^-$ -high pore water in the study area were 55.10 mg/L and 0.07 mg/L, respectively, which were significantly higher than the average sulfate concentration in  $\text{F}^-$ -poor pore water (46.57 mg/L) and lower than the average concentration of barium (0.19 mg/L).

As shown in Figure 5b, PC3 in the fissure water chemistry was characterized by strong positive loadings of fluoride and strontium, weak positive loadings of sodium, and weak negative loadings of nitrate. The fact that fluoride, strontium, and sodium were located in the same factor and were all positively loaded suggested that this observation may be due to homologous relationships or associated geochemical interactions. On the one hand, considering that minerals rich in fluoride, strontium, and sodium were extremely rare, the possibility of a homologous relationship was presumed to be low; on the other hand, the analysis in the above section considered that soil fluoride leaching by long-term agricultural irrigation may be one of the main sources of  $\text{F}^-$ -high fissure water in the study area. Previous studies have shown that continuous irrigation not only leaches fluoride from the soil but also promotes cation exchange in the soil [16,22], resulting in relatively easy-to-fix cations such as calcium ions being fixed from the irrigation water into the soil medium and replacing relatively difficult-to-fix metal ions such as sodium and strontium ions [23], which ultimately led to the enrichment of fluoride, strontium, and sodium in the groundwater by leaching from the soil layer under the effect of long-term irrigation. Correspondingly, the fluoride and sodium and strontium content in the fissure water of the study area showed highly significant positive correlations (Figure 7).

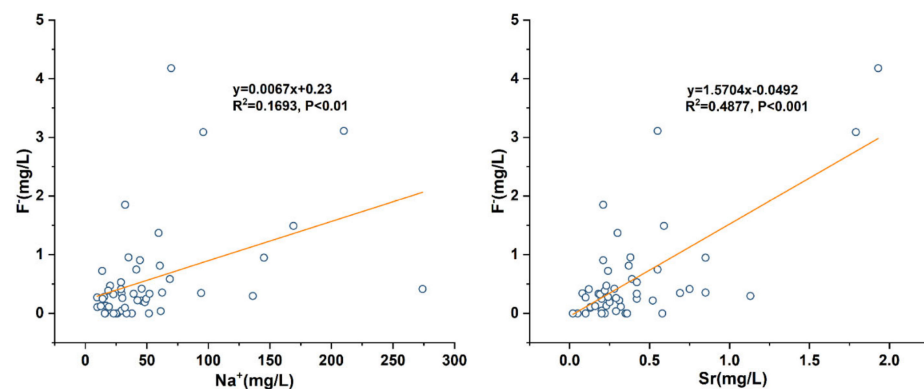


Figure 7. Relationship between the concentrations of  $\text{F}^-$  and  $\text{Na}^+$  and Sr in fissure water.

## 6. Conclusions

In this paper, the occurrence of  $F^-$  in groundwater in the western coastal area of Hainan Island was investigated.  $F^-$ -high ( $>1$  mg/L) groundwater accounted for about 5% of the total groundwater distribution in the study area, mainly in the eastern part of Sanjia town, the southwestern part of Shiyuetian town, and the southeastern part of Wulie town. The proportion of  $F^-$ -high groundwater in FW was 12.2%, which was about two times that in PW. The PFHG of PW in decreasing order was woodland  $>$  cultivated land  $>$  construction land. And the PFHG of FW in decreasing order was cultivated land  $>$  construction land  $>$  woodland  $>$  grassland.

Fluoride in pore water in this study was mainly due to fluoride/aluminum-containing minerals such as phlogopite and calcite in the vadose zone, which are affected by leaching and dissolve in groundwater, thus showing the characteristics of co-enrichment of fluoride and aluminum in pore water. The higher concentration of fluoride in fissure water was mainly influenced by the leaching effect of fluoride-containing fertilizers. Continuous irrigation also promotes the cation exchange of sodium, strontium, and calcium, which ultimately manifests itself in high-fluoride fissure water accompanied by high concentrations of sodium and strontium.

Considering the groundwater fluoride contamination in the western coastal area of Hainan Island revealed in this study, it is recommended that fluoride-containing fertilizers be applied reasonably and that excessive application of fertilizers be limited; additionally, monitoring of groundwater quality in the region should be strengthened to ensure the environmental safety of drinking water sources.

**Supplementary Materials:** The following supporting information can be downloaded at: <https://www.mdpi.com/article/10.3390/w15203678/s1>. Table S1: The coefficients of variation of  $F^-$ -high groundwater; Figure S1: Hydrogeological profile of the study area; Figure S2: Land-use types in the study area.

**Author Contributions:** Conceptualization, R.L.; methodology, R.L. and X.L.; software, X.Y.; validation, R.L., X.L., X.Y. and M.Z.; formal analysis, R.L.; investigation, M.Z.; resources, X.L.; data curation, R.L.; writing—original draft preparation, R.L.; writing—review and editing, X.L.; visualization, X.Y.; supervision, M.Z. All authors have read and agreed to the published version of the manuscript.

**Funding:** This research was funded by the China Geological Survey grant number No. ZD20220209, and the China Geological Survey grant number DD20230507.

**Data Availability Statement:** Not applicable.

**Conflicts of Interest:** The authors declare that they have no conflict of interest.

## References

1. Jha, P.K.; Tripathi, P. Arsenic and fluoride contamination in groundwater: A review of global scenarios with special reference to India. *Groundw. Sustain. Dev.* **2021**, *13*, 100576. [[CrossRef](#)]
2. Jadhav, S.V.; Bringas, E.; Yadav, G.D.; Rathod, V.K.; Ortiz, I.; Marathe, K.V. Arsenic and fluoride contaminated groundwaters: A review of current technologies for contaminants removal. *J. Environ. Manag.* **2015**, *162*, 306–325. [[CrossRef](#)]
3. Cherry, J. The Groundwater Project: Democratizing Groundwater Knowledge. *Groundwater* **2020**, *58*, 682–683. [[CrossRef](#)] [[PubMed](#)]
4. Hao, A.B.; Zhang, Y.L.; Zhang, E.Y.; Li, Z.H.; Yu, J.; Wang, H.; Yang, J.F.; Wang, Y. Review: Groundwater resources and related environmental issues in China. *Hydrogeol. J.* **2018**, *26*, 1325–1337. [[CrossRef](#)]
5. Gleeson, T.; Cuthbert, M.; Ferguson, G.; Perrone, D. Global Groundwater Sustainability, Resources, and Systems in the Anthropocene. *Annu. Rev. Earth Planet. Sci.* **2020**, *48*, 431–463. [[CrossRef](#)]
6. Gleeson, T.; Richter, B. How much groundwater can we pump and protect environmental flows through time? Presumptive standards for conjunctive management of aquifers and rivers. *River Res. Appl.* **2018**, *34*, 83–92. [[CrossRef](#)]
7. Medici, G.; Langman, J.B. Pathways and Estimate of Aquifer Recharge in a Flood Basalt Terrain; A Review from the South Fork Palouse River Basin (Columbia River Plateau, USA). *Sustainability* **2022**, *14*, 11349. [[CrossRef](#)]
8. Khatri, N.; Tyagi, S. Influences of natural and anthropogenic factors on surface and groundwater quality in rural and urban areas. *Front. Life Sci.* **2015**, *8*, 23–39. [[CrossRef](#)]

9. Zhang, L.Q.; Dong, D.L.; Lv, S.T.; Ding, J.; Yan, M.H.; Han, G.L. Spatial evolution analysis of groundwater chemistry, quality, and fluoride health risk in southern Hebei Plain, China. *Environ. Sci. Pollut. Res.* **2023**, *30*, 61032–61051. [[CrossRef](#)] [[PubMed](#)]
10. Liu, C.Y.; Hou, Q.X.; Chen, Y.T.; Huang, G.X. Hydrogeochemical Characteristics and Groundwater Quality in a Coastal Urbanized Area, South China: Impact of Land Use. *Water* **2022**, *14*, 4131. [[CrossRef](#)]
11. Huang, G.X.; Hou, Q.X.; Han, D.Y.; Liu, R.A.; Song, J.M. Large scale occurrence of aluminium-rich shallow groundwater in the Pearl River Delta after the rapid urbanization: Co-effects of anthropogenic and geogenic factors. *J. Contam. Hydrol.* **2023**, *254*, 104130. [[CrossRef](#)] [[PubMed](#)]
12. Huang, G.X.; Liu, C.Y.; Li, L.P.; Zhang, F.G.; Chen, Z.Y. Spatial distribution and origin of shallow groundwater iodide in a rapidly urbanized delta: A case study of the Pearl River Delta. *J. Hydrol.* **2020**, *585*, 124860. [[CrossRef](#)]
13. Huang, G.X.; Pei, L.X.; Li, L.P.; Liu, C.Y. Natural background levels in groundwater in the Pearl River Delta after the rapid expansion of urbanization: A new pre-selection method. *Sci. Total Environ.* **2022**, *813*, 151890. [[CrossRef](#)]
14. Kumar, M.; Goswami, R.; Patel, A.K.; Srivastava, M.; Das, N. Scenario, perspectives and mechanism of arsenic and fluoride Co-occurrence in the groundwater: A review. *Chemosphere* **2020**, *249*, 126126. [[CrossRef](#)] [[PubMed](#)]
15. Kim, Y.; Kim, J.Y.; Kim, K. Geochemical characteristics of fluoride in groundwater of Gimcheon, Korea: Lithogenic and agricultural origins. *Environ. Earth Sci.* **2011**, *63*, 1139–1148. [[CrossRef](#)]
16. Young, S.M.; Pitawala, A.; Ishiga, H. Factors controlling fluoride contents of groundwater in north-central and northwestern Sri Lanka. *Environ. Earth Sci.* **2011**, *63*, 1333–1342. [[CrossRef](#)]
17. Driscoll, C.T.; Schecher, W.D. The Chemistry of Aluminum in the Environment. *Environ. Geochem. Health* **1990**, *12*, 28–49. [[CrossRef](#)]
18. Selinus, O. Fluoride in Natural Waters. In *Essentials of Medical Geology*; Academic Press: Cambridge, MA, USA, 2013; pp. 311–336.
19. Marandi, A.; Karro, E.; Puura, E. Barium anomaly in the Cambrian-Vendian aquifer system in North Estonia. *Environ. Geol.* **2004**, *47*, 132–139. [[CrossRef](#)]
20. Underwood, E.C.; Ferguson, G.A.; Betcher, R.; Phipps, G. Elevated Ba concentrations in a sandstone aquifer. *J. Hydrol.* **2009**, *376*, 126–131. [[CrossRef](#)]
21. Bondu, R.; Cloutier, V.; Rosa, E.; Roy, M. An exploratory data analysis approach for assessing the sources and distribution of naturally occurring contaminants (F, Ba, Mn, As) in groundwater from southern Quebec (Canada)—ScienceDirect. *Appl. Geochem.* **2020**, *114*, 104500. [[CrossRef](#)]
22. Huang, G.X.; Sun, J.C.; Zhang, Y.; Chen, Z.Y.; Liu, F. Impact of anthropogenic and natural processes on the evolution of groundwater chemistry in a rapidly urbanized coastal area, South China. *Sci. Total Environ.* **2013**, *463*, 209–221. [[CrossRef](#)] [[PubMed](#)]
23. Kaleem, M.; Naseem, S.; Bashir, E.; Shahab, B.; Rafique, T. Discrete geochemical behavior of Sr and Ba in the groundwater of Southern Mor Range, Balochistan, a tracer for igneous and sedimentary rocks weathering and related environmental issues. *Appl. Geochem.* **2021**, *130*, 104996. [[CrossRef](#)]

**Disclaimer/Publisher’s Note:** The statements, opinions and data contained in all publications are solely those of the individual author(s) and contributor(s) and not of MDPI and/or the editor(s). MDPI and/or the editor(s) disclaim responsibility for any injury to people or property resulting from any ideas, methods, instructions or products referred to in the content.